Two-dimensional Fermionic Hong-Ou-Mandel Interference with Weyl Fermions

M. A. Khan[1,2,3], Michael N. Leuenberger[1,2]
[1] *NanoScience Technology Center, University of Central Florida, Orlando, Florida 32826, USA*
[2] *Department of Physics, University of Central Florida, Orlando, Florida 32816, USA. and*
[3] *Federal Urdu University of Arts, Science and Technology, Islamabad, Pakistan.*

We propose a two-dimensional Hong-Ou-Mandel (HOM) type interference experiment for Weyl fermions in graphene and 3D topological insulators. Since Weyl fermions exhibit linear dispersion, similar to photons in vacuum, they can be used to obtain the HOM interference intensity pattern as a function of the delay time between two Weyl fermions. We show that while the Coulomb interaction leads to a significant change in the angle dependence of the tunneling of two identical Weyl fermions incident from opposite sides of a potential barrier, it does not affect the HOM interference pattern, in contrast to previous expectations. We apply our formalism to develop a Weyl fermion beam-splitter (BS) for controlling the transmission and reflection coefficients. We calculate the resulting time-resolved correlation function for two identical Weyl fermions scattering off the BS.

arXiv:1405.5312v1 [cond-mat.mes-hall] 21 May 2014

When two indistinguishable bosons are incident on opposite sides of a 50/50 BS, Bose-Einstein quantum statistics demands bunching, i.e. the outgoing bosons must leave together in one of the two outputs, which was first observed with photons in the HOM experiment.[1] Observation of zero coincidence for simultaneous photons is identified by a dip in the correlation function and rises with time delay.[1] HOM type interference has been utilized in quantum tests of non-locality[2] and can be used to investigate the degree of indistinguishability of the incident particles. Also, the HOM experiment is one of the key elements of linear-optics based quantum computation.[3] Several experiments have already demonstrated the HOM interference with photons,[1,4] plasmons,[5] levitons,[6] and electrons.[7–9] Interestingly, it is possible to replace the bosons in the HOM interference experiment by fermions, which leads to the exactly opposite behavior. Due to the Fermi-Dirac quantum statistics fermions appear in different outputs as identical fermions have the tendency of antibunching over small distances, leading to a peak in the coincidence measurement at zero delay. While photons in vacuum exhibit linear dispersion relation, electrons in gapped semiconductor materials typically have a quadratic dispersion relation, which is a major obstacle for observing the fermionic analogue of the HOM interference due to the spreading of electronic wavefunction. In order to overcome this obstacle, it is essential to identify physical systems where the electrons have linear dispersion relation.

One such example is the one-dimensional edge states of quantum Hall systems exhibiting ballistic conductance and linear dispersion, where the one-dimensional fermionic HOM experiment[9] has been successfully implemented. Similar results are expected theoretically for quantum spin Hall states.[10] In order to create a two-dimensional fermionic HOM interference pattern, we need fermionic particles with a linear dispersion relation in two dimensions. Ideal candidates are Weyl fermions in graphene[11,12] and on the surface of 3D topological insulators.[13] Here we show that it is possible to create two-dimensional fermionic HOM interference pattern by considering the scattering of two Weyl fermions in the case of a rectangular potential barrier. We show that at specific incident angles a 50/50 BS for Weyl fermions can be realized, even when considering the Coulomb interaction between the Weyl fermions. Interestingly, the Coulomb interaction leads to a substantial change in angle distribution of the transmission and reflection coefficients. In Ref. 9 a quantum point contact is used as a 50/50 BS for the electrons. The reduction in the correlation function at zero time delay is attributed to the Coulomb interaction between the electrons.[9] Here we show that the Coulomb interaction does not affect the correlation function, i.e. the correlation function is determined solely by the quantum statistics of the particles.

The realization of fermionic HOM interference experiment is provided by a three-step process: (i) Generation of single electron source. (ii) Construction of BS, which is the primary focus of this work. (iii) Detector for counting the coincidences. In solid state devices a single electron transistor (SET) can be used as a source of producing single electrons or a sequential electron gun.[14] The SET consists of a source in the form of a quantum dot tunnel coupled to a conductor through a quantum point contact. By applying a sudden voltage step on a capacitively coupled gate, the charging energy is compensated for and the electron occupying the highest energy level of the dot is emitted. The final state of the electron is a coherent wave packet propagating away in the conductor. Its energy width is given by the inverse tunneling time. The absence of an energy gap in 2-D graphene and phenomena related to Klein tunneling[15] make it hard to confine carriers electrostatically and to control transport on the level of single particles. However, by focusing on armchair graphene nanoribbons, which are known to exhibit an energy gap due to boundary conditions,[16–18] this limitation can be overcome. It has been shown that such an energy gap allows to fabricate tunable graphene nanodevices.[19,20] Particularly, in Ref. 20 it was shown that quantum dots in graphene over a size of 100 nm behave as conventional single electron transistors and exhibit Coulomb blockade.

It was shown[15] that the transmission probability T of

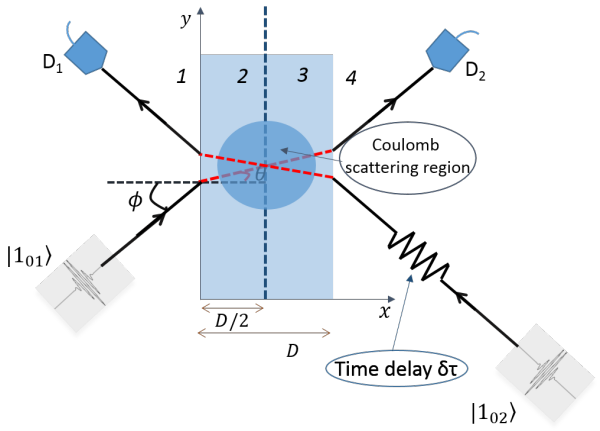


Figure 1: HOM experiment with Weyl fermion BS.

Weyl fermions (in graphene) with energy E through a rectangular potential barrier of height V_0 and width D varies as a function of incident angle ϕ. 100% transmission probability is observed at normal incidence $\phi = 0$, a feature known as Klein tunneling. Exactly the same result can be obtained for surface electronic states of 3D topological insulators. The reason for this coincidence is that in both systems the dynamics of electrons is defined by similar Hamiltonians. The only difference between the two systems is that in graphene the pseudo-spin is locked parallel to the linear momentum and in 3D topological insulators the real spin is locked perpendicular to linear momentum, respectively, i.e

$$\hat{H}_{0,g} = v_F \boldsymbol{\sigma}\cdot\mathbf{p},\ \hat{H}_{0,TI} = v_{eff}(\boldsymbol{\sigma}\times\mathbf{p}), \tag{1}$$

where σ_i's are Pauli matrices, corresponding to the pseudo-spin in the case of graphene and to the real spin in the case of 3D topological insulators, respectively, and $\mathbf{p}$ is the momentum operator. The angle dependent transmission probability through a potential barrier can be used to make a BS for Weyl fermions. For observing the HOM type interference we need to inject two Weyl fermions from the opposite sides of the barrier as shown in Fig. 1 and their transmissions and reflections will produce the desired interference.

We take advantage of the eikonal approximation[21] to calculate the phase change acquired by a Weyl electron when scattering from a second Weyl electron due to the Coulomb interaction. We choose the barrier potential height in such a way that inside the barrier the Coulomb scattering potential $V(r)$ is small compared to the kinetic energy of the incident electrons. Although we solve the Coulomb scattering for Weyl fermions in graphene, our results are general and applicable to surface states of 3D topological insulators as well. Working in the eikonal approximation the exact wave function Ψ of the Hamiltonian $H = H_0 + V(r)$ can be approximated by a semi-classical wave function

$$\Psi \sim \begin{pmatrix} a \\ b \end{pmatrix} e^{iS(r)/\hbar}. \tag{2}$$

Starting from the Dirac equation shown in eq. (1) and expanding in powers of $\hbar$, we obtain in zeroth order the relativistic Hamilton-Jacobi equation

$$|\partial_x S(r)|^2 + |\partial_y S(r)|^2 \approx E^2/v_F^2 - 2V(r)E/v_F^2. \tag{3}$$

We compute $S(r)$ from Eq. 3 by assuming that the trajectory is a straight line, which is valid for large energies and small deflection angles.[21] Eq. 3 then yields in linear approximation in V

$$\frac{S(x)}{\hbar} \approx kx - \frac{1}{\hbar v_F}\int_{-\infty}^{x} 2V(b,x')dx'. \tag{4}$$

Similar to the non-relativistic derivation,[21] we obtain the relativistic scattering amplitude

$$f(\mathbf{k},\mathbf{k}') = -i\sqrt{\frac{k}{2\pi}}\int_{-\infty}^{\infty} db e^{-ikb\theta}\left[e^{2i\triangle(b)} - 1\right], \tag{5}$$

where $\triangle(b) = -\frac{1}{2\hbar v_F}\int_{-\infty}^{\infty} dx' V(b,x')$ and θ is the angle between $\mathbf{k}$ and $\mathbf{k}'$. Eq. 5 is in agreement with the optical theorem in scattering theory.[21] Eq. (5) can be solved for the screened Coulomb potential, i.e. the Yukawa potential with $V(b,x') = U_0 \exp\left(-\mu\sqrt{b^2+x^2}\right)/\mu\sqrt{b^2+x^2}$, where μ^{-1} is the screening length, for graphene $\mu = g_s g_v e^2 k_F/\kappa\hbar v_F$, κ is the background lattice dielectric constant, $U_0 = e^2\mu/4\pi\kappa\epsilon_0$, and k_F is the Fermi wave vector. In the lab frame $\theta \longrightarrow \theta/2$. The phase change Δ in the forward direction acquired by the particle while passing through the scattering region can be evaluated by setting $|\mathbf{k}| = |\mathbf{k}'| = k_F$ for elastic scattering, i.e.

$$\Delta = \lim_{\theta\longrightarrow 0} Re\left(\sqrt{k_F} f(\mathbf{k},\mathbf{k}')\right) = -\frac{\sqrt{2\pi}U_0}{\hbar v_F \mu}\frac{k_F}{\mu}. \tag{6}$$

It is now straightforward to solve the tunneling problem shown in Fig. 1. The electron is incident on the barrier from right at an angle ϕ with respect to the x axis. It propagates at an angle θ in region 2 and is transmitted in region 3 at the same angle ϕ. Using the notation in Ref. 15, the components of the Weyl spinor Ψ_1 and Ψ_2 can be written as $\Psi_i(x,y) = \Psi_i(x)e^{ik_y y}$, $i = 1,2$, with

$$\Psi_1(x) = \begin{cases} e^{ik_x x} + re^{-ik_x x} & x < 0 \\ ae^{iq_x x} + be^{-iq_x x} & 0 < x < \frac{D}{2} \\ ae^{iq_x x + i\Delta} + be^{-iq_x x - i\Delta} & \frac{D}{2} < x < D \\ te^{ik_x x + i\Delta} & x > D \end{cases}, \tag{7}$$

$$\Psi_2(x) = \begin{cases} s\left[e^{ik_x x + i\phi} - re^{-ik_x x - i\phi}\right] & x < 0 \\ s'\left[ae^{iq_x x + i\theta} - be^{-iq_x x - i\theta}\right] & 0 < x < \frac{D}{2} \\ s'\left[ae^{iq_x x + i\theta + i\Delta} - be^{-iq_x x - i\theta - i\phi}\right] & \frac{D}{2} < x < D \\ ste^{ik_x x + i\phi + i\Delta} & x > D \end{cases} \tag{8}$$

where $k_x = k_F\cos\phi, k_y = k_F\sin\phi$ are the components of the wavevector outside the barrier and $q_x =$

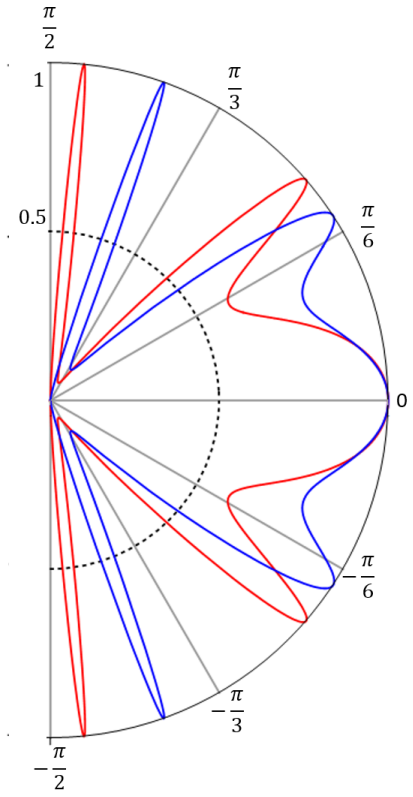


Figure 2: Transmission probability T as a function of incident angle ϕ. The electron concentration n outside the barrier is chosen as 0.5×10^{12} cm^{-2}. This corresponds to a Fermi energy and wavelength of incident electrons of $E_F \approx 80$ meV and $\lambda \approx 50$ nm, respectively. The barrier height $V_0 = 200$ meV. The red curve is the solution for $\Delta = 0$ and the blue curve is the solution for $\Delta = -0.63$. Black (dashed) semicircle is drawn at 50% transmission probability.

$\sqrt{(E-V_0)^2/(\hbar v_F)^2 - k_y^2}$ and $\tan\theta = k_y/q_x$. The transmission coefficient$t$ can be evaluated by using the continuity conditions at $x = 0$ and $x = D$ and is

$$t = 2\exp(-ik_xD)\cos\theta\cos\phi/\left\{ss'\left[e^{-i(q_xD+\Delta)}\cos(\theta+\phi) + e^{i(q_xD+\Delta)}\cos(\theta-\phi)\right] - 2i\sin(q_xD+\Delta)\right\}. \quad (9)$$

In Fig. 2 the transmission coefficient $T = t^*t$ is plotted as a function of incident angle ϕ for the cases when Δ=0 (red curve) and $\Delta = -\sqrt{2\pi}U_0k_F/\hbar v_F\mu^2$ (blue curve). Interestingly, the Coulomb interaction results in a substantial shift of the transmission peaks while preserving Klein tunneling. In the limit $V_0 \ll E$,

$$T = \frac{cos^2\phi}{1 - cos^2(q_xD+\Delta)sin^2\phi}. \quad (10)$$

For normal incidence T is always 1, regardless of the height and width of the barrier. Away from normal incidence, the other transmission peaks correspond to the condition of constructive interference, which occurs when $q_xD+\Delta = n\pi$ where $n = 0, \pm1, \pm2, ...$ Comparing Eq. (10) with the result in Ref. 15, there is an additional phase Δ in the denominator, which comes from the Coulomb interaction. It can be seen from Fig. 2 that at certain angles the transmission coefficient is 50%. For these angles of incidence this modified barrier can be used as a 50/50 BS. At the same ϕ, the Coulomb interaction then leads to an asymmetry in T and R. In addition, we can change the transmission and reflection coefficients to any desired value ranging between 0 and 1 by tuning ϕ.

The schematic diagram of the HOM experiment is shown in Fig. 1. It consists of two SET's as the sources of the two electrons, a BS (orange line) and electron counters (blue pentagons).[22,23] The BS is considered to be lossless, i.e. $T + R = 1$. Let us now consider two Weyl fermions that are incident on the BS from opposite sides. Let τ_1 be the time it takes for the electrons to get from the source to the detector. We define $\delta\tau$ as the time delay between the two incident electrons. $\delta\tau$ can be introduced either by displacing the position of the BS towards one of the sources or by introducing the time delay between the switching pulses of the two SET's. Our goal is to calculate the correlation function corresponding to the coincidence counts at the two detectors as a function of the time delay $\delta\tau$. The inputs of the BS are described by the indices 01,02 i.e. $c_{01}^\dagger|0_{01},0_{02}\rangle = |1_{01},0_{02}\rangle$and $c_{02}^\dagger|0_{01},0_{02}\rangle = |0_{01},1_{02}\rangle$, where $c_{01}^\dagger(c_{01})$ are electron creation (annihilation) operators. We omit the spin index because we assume that the two electrons have parallel spins. Similarly, the outputs are described by the indices 1, 2. The output operators are related to the input operators through the following linear scattering relations

$$\hat{c}_1(t) = \sqrt{T}\hat{c}_{01}(t-\tau_1) + i\sqrt{R}\hat{c}_{02}(t-\tau_1+\delta\tau), \quad (11)$$
$$\hat{c}_2(t) = \sqrt{T}\hat{c}_{02}(t-\tau_1) + i\sqrt{R}\hat{c}_{01}(t-\tau_1-\delta\tau), \quad (12)$$

where i corresponds to a $\pi/2$ phase shift and $\hat{c}_{0j}(t) = \xi_j(t)\hat{c}_{02}$. $\xi_j(t)$ is the distribution function in time. Electrons emitted from the SET usually follow an exponential profile in time, i.e. $\xi_j(t) = \Theta(t)\exp(-\Gamma_jt/2)\exp(i\omega t)$.[9] $\Theta(t)$ is the Heavyside step function and $\Gamma_j$is the SET emission rate of the electron. The correlation function describing the joint probability of detection of electrons at the two detectors at times t and $t+\tau$ is

$$P_{12}(t) = C\left\langle 0\left|\hat{c}_{02}\hat{c}_{01}\hat{c}_1^\dagger(t)\hat{c}_2^\dagger(t+\tau)\hat{c}_2(t+\tau)\hat{c}_1(t)\hat{c}_{01}^\dagger\hat{c}_{02}^\dagger\right|0\right\rangle. \quad (13)$$

C is the normalization constant. This can readily be evaluated by means of Eqs. (11) and (12). The number of coincidence counts $N_c(1,2)$ can be obtained by integrating $P_{12}(t)$ over time t. This yields

$$\frac{N_c(\delta\tau)}{C}\Gamma_1\Gamma_2 = \widetilde{N}_c(\delta\tau) = T^2 + R^2 + RT\frac{8\Gamma_1^2\Gamma_2^2}{(\Gamma_1+\Gamma_2)^2} \times\{\exp(\Gamma_1\delta\tau)\Theta(-\delta\tau) + \exp(-\Gamma_2\delta\tau)\Theta(\delta\tau)\}, \quad (14)$$

where $\widetilde{N}_c(\delta\tau)$ is the normalized number of coincidences. Eq. (14) is our main result. The coincidence counts

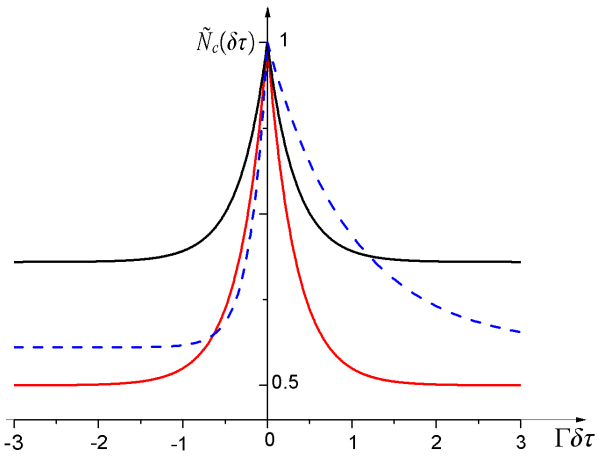


Figure 3: Interference peak for normalized number of coincidences $\widetilde{N}_c(\delta\tau)$ against time delay $\delta\tau$. Red curve is for R=T=1/2 and for $\Gamma_1 = \Gamma_2 = \Gamma$, black curve is for $R = 1/5, T = 4/5$ and for $\Gamma_1 = \Gamma_2 = \Gamma$. Blue curve is for $T = 1/3, R = 2/3$ and$\Gamma_1 = 5\Gamma/3, \Gamma_2 = \Gamma/3$, where $\Gamma = 10^{-12}s^{-1}$.

depend both on the time delay $\delta\tau$ and the transmission and reflection coefficients. The coincidence counts can be tuned by introducing an asymmetry in the reflection and transmission coefficients. For perfect transmissions and reflections $\widetilde{N}_c(\delta\tau)$ remains at unity regardless of the value of $\delta\tau$. For large $\delta\tau$ the third term on the right hand side of Eq. (14) goes to zero, and the expression for the coincidence counts reduces to $T^2 + R^2$. In case of identical electron sources, i.e. $\Gamma_1 = \Gamma_2$, Eq. (14) can be simplified to

$$\begin{aligned}\widetilde{N}_c(\delta\tau) &= T^2 + R^2 + 2RT\left\{\exp(\Gamma_1\delta\tau)\Theta(-\delta\tau)\right. \\ &\quad \left. + \exp(-\Gamma_2\delta\tau)\Theta(\delta\tau)\right\}. \qquad (15)\end{aligned}$$

Note that for $\delta\tau = 0$ $\widetilde{N}_c(\delta\tau) = (T + R)^2 = 1$, no matter what the values of T and R are, which reflects the anti-bunching of fermions. In Fig. 3 we plot the coincidence counts for different R and T and for different values of Γ's (blue) as a function of the time delay $\delta\tau$. Note that, in contrast to the expectation in Ref. 9, the Coulomb interaction does not reduce the peak at $\delta\tau = 0$.

In conclusion, we developed the theoretical model of the two-dimensional HOM type interference with Weyl fermions in graphene and in 3D topological insulators. The two-dimensional setup allows for the tuning of the transmission and reflection coefficients by varying the angle of incidence of the two Weyl fermions. We provide the description a realistic BS for Weyl fermions, including the effects of Coulomb interaction. Our results show that the Coulomb interaction does not affect the fermionic HOM peak (Pauli peak) for Weyl fermions within the eikonal approximation. We conjecture that as long as the detectors can absorb electrons laterally spread by the Coulomb interaction, our results are valid beyond the eikonal approximation.

Acknowledgments. We acknowledge support from NSF (grant ECCS-0901784), AFOSR (grant FA9550-09-1-0450), and NSF (grant ECCS-1128597).

[1] C. K. Hong, , Z. Y. Ou, L. Mandel, Phys. Rev. Lett. **59**, 2044-2046 (1987)

[2] J. Torgerson, D. Branning, C. Monken, and L. Mandel, Phys. Lett. A **204**, 323 (1995).

[3] E. Knill, R. Laflamme, G. J. Milburn, Nature **409**, 46 (2001).

[4] J. Beugnon, M. P. A. Jones, J. Dingjan, B. Darquié, G. Messin, A. Browaeys, P. Grangier, Nature **440**, 779-782 (2006).

[5] Reinier W. Heeres, Leo P. Kouwenhoven, Valery Zwiller, Nature Nanotechnology **8**, 719-722 (2013).

[6] J. Dubois, T. Jullien, F. Portier, P. Roche, A. Cavanna, Y. Jin, W. Wegscheider, P. Roulleau, D. C. Glattli, Nature **502**, 659-663 (2013).

[7] J. R. Petta, H. Lu, A. C. Gossard, Science **327**, 669 (2010).

[8] Guido Burkard, Science **327**, 650 (2010).

[9] E. Bocquillon, V. Freulon, J.-M Berroir, P. Degiovanni, B. Plaçais, A. Cavanna, Y. Jin, G. Fève, Science **339**, 1054 (2013).

[10] D. Ferraro, C. Wahl, J. Rech, T. Jonckheere, T. Martin, Phys. Rev. B **89**, 075407 (2014).

[11] A. K. Geim, K. S. Novoselov, Nature Materials **6**, 183 - 191 (2007).

[12] A. H. Castro Neto, F. Guinea, N. M. R. Peres, K. S. Novoselov, A. K. Geim, Rev. Mod. Phys. **81**, 109-162 (2009).

[13] Haijun Zhang, Chao-Xing Liu, Xiao-Liang Qi, Xi Dai, Zhong Fang and Shou-Cheng Zhang, Nature Physics **5**, 438 - 442 (2009).

[14] G. Fève, A. Mahé, J.-M. Berroir, T. Kontos, B. Plaçais, D. C. Glattli, A. Cavanna, B. Etienne, Y. Jin, Science **316**, 1169 (2007).

[15] M. I. Katsnelson, K. S. Novoselov, amd A. K. Geim, Nature Phys. **2**, 620-625 (2006).

[16] M. Y. Han, B. Özyilmaz, Y. Zhang, and P. Kim, Phys. Rev. Lett. **98**, 206805 (2007).

[17] F. Sols, F. Guinea and A. H. Castro Neto, Phys. Rev. Lett. **99**, 166803 (2007).

[18] X. Li, X. Wang, L. Zhang, S. Lee, H. Dai, Science **319**, 1229 (2008).

[19] C. Stampfer, J. Göttinger, F. Molitor, D. Graf, T. Ihn, and K. Ensslin, Appl. Phys. Lett. **92**, 012102 (2008).

[20] L. A. Ponomarenko, F. Schedin, M. I. Katsnelson, R. Yang, E. W. Hill, K. S. Novoselov, A. K. Geim, Science **320**, 356 (2008).

[21] J. J. Sakurai, Modern Quantum Mechanics, 1994.

[22] Toshimasa Fujisawa, Toshiaki Hayashi, Ritsuya Tomita, Yoshiro Hirayama, Science **312**, 1634 (2006).

[23] Y. Utsumi, D. S. Golubev, M. Marthaler, K. Saito, T. Fujisawa, and Gerd Schön, Phys. Rev. B **81**, 125331 (2010).